



Scholars Research Library

Der Pharma Chemica, 2014, 6(3):6-16
(<http://derpharmachemica.com/archive.html>)



ISSN 0975-413X
CODEN (USA): PCHHAX

2-(2-hydroxyethyl)-6-phenylpyridazin-3(2H)-one as corrosion inhibitor for mild steel in hydrochloric acid solution

A. Ghazoui ^{*1}, H. Tayebi ², N. Benchat ¹, A. Zarrouk ¹, B. Hammouti ¹, R. Salghi ³, A. Guenbour ², R. Touzani ^{1,4}

¹ LCAE-URAC18, Faculté des Sciences, Université Mohammed Premier B.P. 717, 60000 Oujda, Morocco.

² Laboratoire d'Electrochimie et de Corrosion, Faculté des Sciences, Rabat, Morocco.

³ Equipe de Génie de l'Environnement et Biotechnologie, ENSA, Université Ibn Zohr, BP1136 Agadir, Morocco.

⁴ Université Mohammed Premier, Faculté Pluridisciplinaire Nador-Morocco.

ABSTRACT

A new compound of corrosion inhibitor namely 2-(2-hydroxyethyl)-6-phenylpyridazin-3(2H)-one (GP1) was synthesized and its inhibiting action on the corrosion of mild steel in 1.0 M hydrochloric acid at 308 K was investigated by various corrosion monitoring techniques. A preliminary screening of the inhibition efficiency was carried out using weight loss measurements. Potentiodynamic polarization and AC impedance methods have been used. Potentiodynamic polarization studies showed that this pyridazin derivative was mixed type inhibitor. The effect of temperature on the corrosion behaviour of mild steel in 1.0 M HCl with the addition of this compound was studied in the temperature range from 308-343K. The adsorption of this inhibitor on mild steel surface from hydrochloric acid obeyed the Langmuir adsorption isotherm.

Keywords: Pyrimidothiazine inhibitor, Carbon steel, HCl, EIS, Polarization.

INTRODUCTION

One of the most vital processes in the field of prevention of corrosion and its control is the use of organic inhibitors. The crucial part in the mechanistic aspect of such inhibitors is the specific interaction between certain functionalities in the inhibitors with the corrosion active centres on the metal surface. Heteroatoms such as nitrogen, oxygen, sulphur present in the inhibitors play a leading role in this interaction by donating their free electron pairs [1-21]. Hence most of the organic compounds containing these heteroatoms generally act as good inhibitors. In addition, compounds with multiple bonds behave as efficient inhibitors due to the availability of π -electrons for interaction with the metal surface. Certain inhibitors possess both the above two features, viz., availability of lone pair from heteroatom as well as π -electrons in the same molecule, and such compounds show extraordinary inhibition characteristics. Corrosion of mild steel is most common type of corrosion in acidic solution. It has practical importance in acid pickling, chemical scale cleaning, in metallurgy, in petrochemical industry etc. Hydrochloric acid is most common type of acid used in the various industries. This leads to the researchers to study the effect of corrosion inhibitors on mild steel in hydrochloric acid solutions. [22-26].

In the present study, the inhibition of corrosion of mild steel in 1.0 M HCl aqueous solution by 2-(2-hydroxyethyl)-6-phenylpyridazin-3(2H)-one (GP1) was investigated using weight loss method and electrochemical techniques. Effect of temperature was studied between 308 and 343 K and determination of activation parameters.

MATERIALS AND METHODS

Materials and inhibitor

The steel used in this study is mild steel with a chemical composition (in wt %) of 0.21 % C, 0.38 % Si, 0.05 % Mn, 0.05 % S, 0.09 % P, 0.01 % Al and the remainder iron (Fe). Pyridazine organic compound (GP1) is synthesized in the laboratory of Organic Chemistry and Physics (LCAE - URAC18), Faculty of Sciences Oujda, Morocco, by Benchat and al. [27, 28]. The chemical structure of pyridazine derivative studied is given in Fig.1.

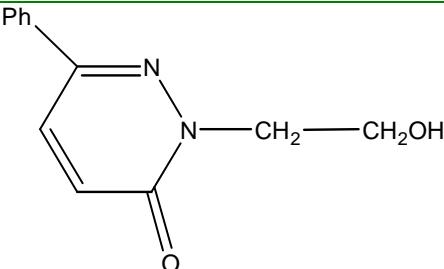
Pyridazine name	Chemical Structure	Abbreviation
2-(2-hydroxyethyl)-6-phenylpyridazin-3(2H)-one		GP1

Figure 1. Chemical name, structure of the pyridazine derivative and their abbreviation

Solutions

The aggressive solutions of 1.0 M HCl were prepared by dilution of analytical grade 37% HCl with distilled water. The organic compound tested is 2-(2-hydroxyethyl)-6-phenylpyridazin-3(2H)-one (GP1). The concentration range of this compound was 10^{-3} to 10^{-6} M.

Weight loss measurements

Coupons were cut into $1 \times 1 \times 0.05$ cm³ dimensions are used for weight loss measurements. Prior to all measurements, the exposed area was mechanically abraded with 180, 320, 800, 1200 grades of emery papers. The specimens were washed thoroughly with bidistilled water, degreased and dried with ethanol. Gravimetric measurements are carried out in a double walled glass cell equipped with a thermostated cooling condenser. The solution volume is 50 mL. The immersion time for the weight loss is 6 h at 308 K. In order to get good reproducibility, parallel triplicate experiments were performed and the average weight loss value of three parallel carbon steel sheets was obtained. The corrosion rate (V) was calculated by the following equation:

$$V = \frac{w}{St} \quad (1)$$

Where V was the corrosion rate in (mg cm⁻² h⁻¹), w is the average weight loss of three parallel carbon steel sheets (mg), S was the total area of one carbon steel sheet (cm²), and t was immersion time (h).

With the calculated corrosion rate, the inhibition efficiency (η_{WL} %) was obtained as the following equation:

$$\eta_{WL} \% = \frac{V_0 - V}{V_0} \times 100 \quad (2)$$

Where V_0 and V are the values of corrosion rate without and with different concentration of inhibitor, respectively.

Polarization measurements

Electrochemical impedance spectroscopy

The electrochemical measurements were carried out using Volta lab (Tacussel- Radiometer PGZ 301) potentiostat and controlled by Tacussel corrosion analysis software model (Voltmaster 4) at under static condition. The corrosion cell used had three electrodes. The reference electrode was a saturated calomel electrode (SCE). A platinum electrode was used as auxiliary electrode of surface area of 0.094 cm². The working electrode was carbon steel. All potentials given in this study were referred to this reference electrode. The working electrode was immersed in test solution for 30 minutes to a establish steady state open circuit potential (E_{ocp}). After measuring the E_{ocp} , the electrochemical measurements were performed. All electrochemical tests have been performed in aerated solutions at 308 K. The EIS experiments were conducted in the frequency range with high limit of 100 kHz and

different low limit 0.1 Hz at open circuit potential, with 10 points per decade, at the rest potential, after 30 min of acid immersion, by applying 10 mV ac voltage peak-to-peak. Nyquist plots were made from these experiments. The best semicircle can be fit through the data points in the Nyquist plot using a non-linear least square fit so as to give the intersections with the x -axis.

The inhibition efficiency of the inhibitor was calculated from the charge transfer resistance values using the following equation [29]:

$$\eta_z \% = \frac{R_{ct(inh)} - R_{ct}}{R_{ct(inh)}} \times 100 \quad (3)$$

where R_{ct} and $R_{ct(inh)}$ were the values of polarization resistance in the absence and presence of inhibitor, respectively.

Potentiodynamic polarization

The electrochemical behaviour of carbon steel sample in inhibited and uninhibited solution was studied by recording anodic and cathodic potentiodynamic polarization curves. Measurements were performed in the 1.0 M HCl solution containing different concentrations of the tested inhibitor by changing the electrode potential automatically from -800 to +200 mV versus corrosion potential at a scan rate of 1 mV s⁻¹. The linear Tafel segments of anodic and cathodic curves were extrapolated to corrosion potential to obtain corrosion current densities (I_{corr}). From the polarization curves obtained, the corrosion current (I_{corr}) was calculated by curve fitting using the equation:

$$I = I_{corr} \left[\exp\left(\frac{2.3\Delta E}{\beta_a}\right) - \exp\left(\frac{2.3\Delta E}{\beta_c}\right) \right] \quad (4)$$

The inhibition efficiency was evaluated from the measured I_{corr} values using the relationship:

$$\eta_{Tafel} \% = \frac{I_{corr}^{\circ} - I_{corr}^i}{I_{corr}^{\circ}} \times 100 \quad (5)$$

where, I_{corr}° and I_{corr}^i are the corrosion current density in absence and presence of inhibitor, respectively.

RESULTS AND DISCUSSION

Gravimetric measurements

Effect of inhibitor concentration

This measurement method allows to directly assessing the corrosion rate (ν), this value can be calculated by equation (1) and subsequently the determination of the effectiveness inhibitory (protective power of an inhibitor (η_{WL} %)) of this organic compound using the relation (2). The value of these parameters obtained from weight loss method at different concentrations of inhibitor in 1.0 M HCl at 308 K temperature is presented in Table 1.

Table 1. Gravimetric results of mild steel in 1.0 M HCl at different concentration of each inhibitor at 6h and 308 K.

Inhibitor	Conc (M)	ν (mg cm ⁻² h ⁻¹)	η_{WL} (%)	θ
Blank	1.0	1.142	-----	-----
	1×10^{-3}	0.185	82.8	0.828
	5×10^{-4}	0.199	82.5	0.825
GP1	1×10^{-4}	0.341	70.0	0.700
	5×10^{-5}	0.435	61.9	0.619
	1×10^{-5}	0.521	54.3	0.543
	1×10^{-6}	0.694	39.1	0.391

From the Table1 and the Fig.2, it is clear that increase of inhibitor concentration caused a decrease in the weight loss as well as corrosion rate of mild steel and, increasing the efficiency of inhibition to reach the maximum value of 82.80% at the highest concentration of 10^{-3} M. This shows that the molecule of GP1 may be adsorbed on the metal surface to cover the active sites on the electrode surface.

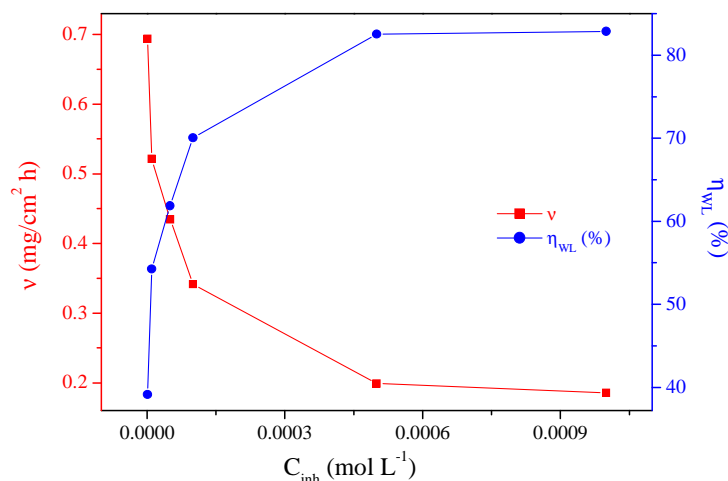


Figure 2. Variation of inhibition efficiency and corrosion rate in 1.0 M HCl on mild steel surface without and with different concentrations of GP1.

Effect of temperature and thermodynamic activation parameters

The effect of temperature on the corrosion rate of carbon steel in 1.0 M HCl over the temperature range (308 to 343 K) (see Table 2) in the absence and presence of different concentrations of the investigated compounds has been studied. The % inhibition efficiency is found to decrease with increasing the temperature; this indicated that, this compound is physically adsorbed on the carbon steel surfaces.

Table 2. Various corrosion parameters for mild steel in 1.0 M HCl in the absence and the presence of optimum concentration of GP1 at different temperatures after 1h.

Temp (K)	Inhibitor	v (mg cm ⁻² h ⁻¹)	η _{WL} (%)	θ
308	Blank	1.142	-----	-----
	GP1	0.185	82.8	0.828
313	Blank	1.580	-----	-----
	GP1	0.330	79.1	0.791
323	Blank	3.030	-----	-----
	GP1	0.944	68.8	0.688
333	Blank	5.150	-----	-----
	GP1	2.374	53.9	0.539
343	Blank	9.000	-----	-----
	GP1	5.713	36.5	0.365

The dependence of corrosion rate at temperature can be expressed by Arrhenius equation and transition state equation:

$$\ln(v) = -\frac{E_a}{RT} + \ln\lambda \quad (6)$$

$$v = \frac{RT}{Nh} \exp\left(\frac{\Delta S_a}{R}\right) \exp\left(-\frac{\Delta H_a}{RT}\right) \quad (7)$$

where v is the corrosion rate, λ the pre-exponential factor, h is the Planck's constant (6.626176×10^{-34} Js), N is the Avogadro's number (6.02252×10^{23} mol⁻¹), R is the universal gas constant and T is the absolute temperature, ΔH_a the enthalpy of activation, and ΔS_a entropy of activation. The apparent activation energy and pre-exponential factors for a 1.0 mM of concentration of the inhibitor can be calculated by linear regression between $\ln(v)$ and $1/T$, the results were shown in Table 3.

A plot shown in Figure 3, of corrosion rate obtained by weight loss measurement versus $1/T$ gave straight line. The value of the E_a obtained from the slope equals to the $(-E_a/R)$ and the pre exponential factor calculates by the intercept

($\ln \lambda$) of the line reported in Table 3. It is evident from the Table 3 that the activation energy increased on addition of GP1 in comparison to the uninhibited solution. The increase in the apparent activation energy value interpreted as the decrease in the inhibition efficiency with the increase in the temperature. This leads to the increase in corrosion rate due to the greater area of metal that is exposed towards the corrosive environment [30].

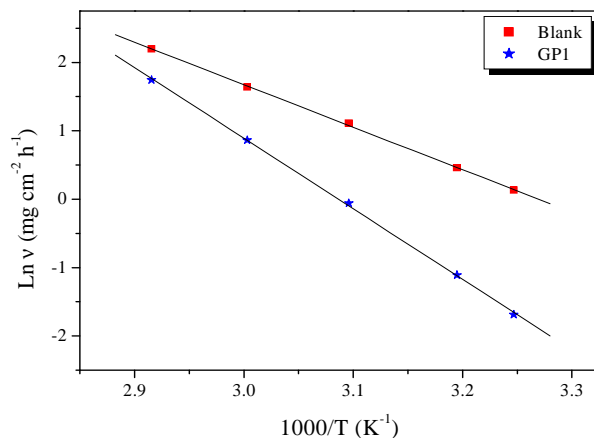


Figure 3. Arrhenius plots of $\ln v$ vs. $1000/T$ for steel in 1.0 M HCl in the absence and the presence of GP1 at optimum concentration.

A plot of $\ln(v/T)$ versus $1/T$ is shown in Figure 4. Straight lines were obtained with slope $(-\Delta H_a/R)$ and intercept of $[\ln(R/Nh) + (\Delta S_a/R)]$, from which ΔH_a and ΔS_a were calculated and listed in Table 3. It is clear from the Table 3 that the entropy of activation increased in the presence of inhibitor in comparison to the uninhibited sample. The increase in the activation entropy in presence of inhibitor indicates the increase in the disorderliness on going from reactant to activated complex. It is evident from the table that the value of ΔH_a increased in the presence of inhibitor than in the uninhibited solution indicating the higher inhibitive efficiency. This may be attributed to the presence of an energy barrier for the reaction, hence, the process of adsorption of inhibitor leads to rise in enthalpy of the corrosion process.

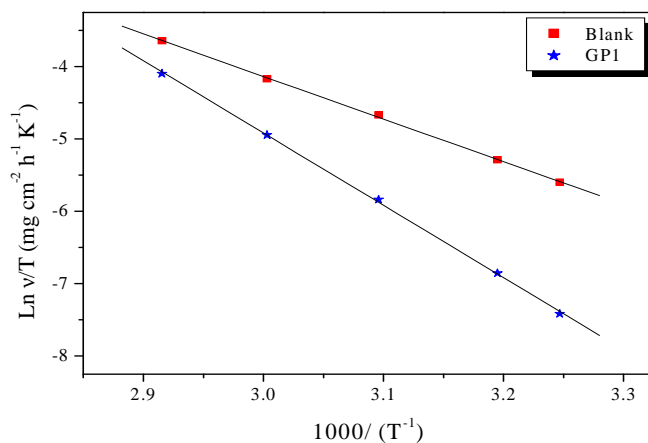


Figure 4. Arrhenius plots of $\ln(v/T)$ vs. $1/T$ for steel in 1.0 M HCl in the absence and the presence of GP1 at optimum concentration.

Table 3 Activation parameters for the steel dissolution in 1.0 M HCl in the absence and the presence of GP1 at 1.0 mM.

Inhibitor	A ($\text{mg cm}^{-2} \text{h}^{-1}$)	Linear regression coefficient (r)	E_a (kJ/mol)	ΔH_a (kJ/mol)	ΔS_a (J/mol K)
Blank	6.6808×10^{08}	0.99976	51.67	48.97	-85.00
GP1	5.1300×10^{13}	0.99991	85.01	82.31	8.53

Adsorption isotherm and thermodynamic parameters

The organic inhibitors are compounds having at least one active center of the chemisorptions (hetero multiple bonds or aromatic rings having π -electrons). In the case of aromatic compounds, the electron density will be affected by the introduction of substituent's, which increases or decreases the corrosion-inhibiting effectiveness. The inhibition of corrosion of metals by organic compounds is explained by their adsorption. The latter is described by two main types of adsorption, namely physical adsorption and chemical adsorption. It depends on the charge of the metal, the nature of the chemical structure of the organic product and the type of electrolyte. The presence of a transition metal, having orbital "d" vacant, and a molecule having centers that facilitates electron rich adsorption [31,32]. Accordingly, the fraction of surface covered with inhibitor species ($\theta = \eta_{WL} \% / 100$) can follow as a function of inhibitor concentration and solution temperature. The surface coverage (θ) data are very useful on discussing the adsorption characteristics. When the fraction of surface covered is determined as a function of the concentration at constant temperature, adsorption isotherm could be evaluated at equilibrium condition. The dependence of the fraction of the surface covered θ on the concentration C_{inh} of the inhibitor was tested graphically by fitting it to Langmuir's isotherm, which assumes that the solid surface contains a fixed number of adsorption sites and each site holds one adsorbed species. Fig. 5 shows the linear plots for C_{inh}/θ versus C_{inh} , suggesting that the adsorption obeys the Langmuir's isotherm:

$$\frac{C_{inh}}{\theta} = \frac{1}{K_{ads}} + C_{inh} \quad (8)$$

where C_{inh} is the inhibitor concentration, and K_{ads} the adsorptive equilibrium constant, representing the degree of adsorption (i.e., the higher value of K_{ads} indicates that the inhibitor is strongly adsorbed on the metal surface); the value of K_{ads} obtained from the reciprocal of intercept of Langmuir plot lines and the slope of these lines is near unity, meaning that each inhibitor molecule occupies one active site on the metal surface. The correlation coefficient (R^2) was used to choose the isotherm that best fit experimental data (Table 4).

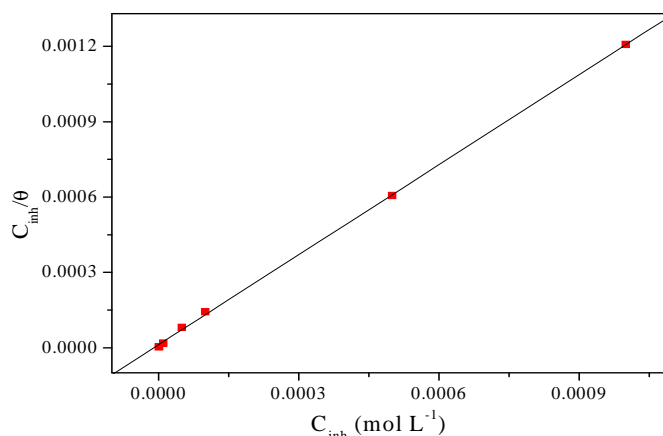


Figure 5. Langmuir adsorption of GPI on the steel surface in 1.0 M HCl solution

From the intercepts of the straight lines on the C_{inh}/θ -axis (Figure 3), K_{ads} can be calculated which is related to free energy of adsorption, ΔG_{ads}° as given by

$$\Delta G_{ads}^{\circ} = -RTL \ln(55.5 K_{ads}) \quad (9)$$

where R is gas constant and T is absolute temperature of experiment and the constant value of 55.5 is the concentration of water in solution in mol L⁻¹.

Table 4. Thermodynamic parameters for the adsorption of GPI in 1.0 M HCl on the mild steel at 308K.

Inhibitor	Slope	K_{ads} (M ⁻¹)	R^2	ΔG_{ads}° (kJ/mol)
GPI	1.19	81742.76	0.99984	-39.27

Generally, the energy values of -20 kJ mol^{-1} or less negative are associated with an electrostatic interaction between charged molecules and charged metal surface, physisorption; those of -40 kJ mol^{-1} or more negative involve charge sharing or transfer from the inhibitor molecules to the metal surface to form a coordinate covalent bond, chemisorption [33,34]. The value of the standard free energy of adsorption $\Delta G_{\text{ads}}^{\circ}$ listed in Table 4, since it is between the values of -40 kJ mol^{-1} and -20 kJ mol^{-1} , allows us to suggest that the adsorption of our inhibitors has two types of interactions: chemisorption and physisorption [14,35].

Electrochemical impedance spectroscopy

Nyquist representation of the EIS study of mild steel in 1.0 M HCl in absence and presence of different concentration of GP1 were presented in figure 6. The large capacitive loop attributed to the adsorption of the inhibitor molecule [36]. The simple equivalent Randle circuit for studies is shown in Fig. 6, where R_s represents the solution and corrosion product film; the parallel combination of resistor, R_{ct} and capacitor C_{dl} represents the corroding interface. The existence of single semi circle showed the single charge transfer process. Depression from the perfect semi circle is due to the inhomogeneous nature of the metal surface arising from the surface roughness or the interfacial phenomenon [37]. The increase in R_{ct} values due to the addition of inhibitor in comparison to the absence of inhibitor is attributed to the formation of protective film on the metal/solution interface. These observations suggest that GP1 molecules function by adsorption at metal surface thereby causing the decrease in C_{dl} values and increase in R_{ct} values [36-38]. The charge transfer resistance (R_{ct}) and the interfacial double layer capacitance (C_{dl}) derived from these curves are given in Table 4. Inhibition efficiency was calculated by the using the charge transfer resistance values. The capacity of the double layer C_{dl} is determined at the frequency at which the imaginary part of the impedance is maximal ($-Z_{\text{max}}$) from the following equation:

$$f(-Z_{\text{max}}) = \frac{1}{2\pi C_{dl} R_{ct}} \quad (10)$$

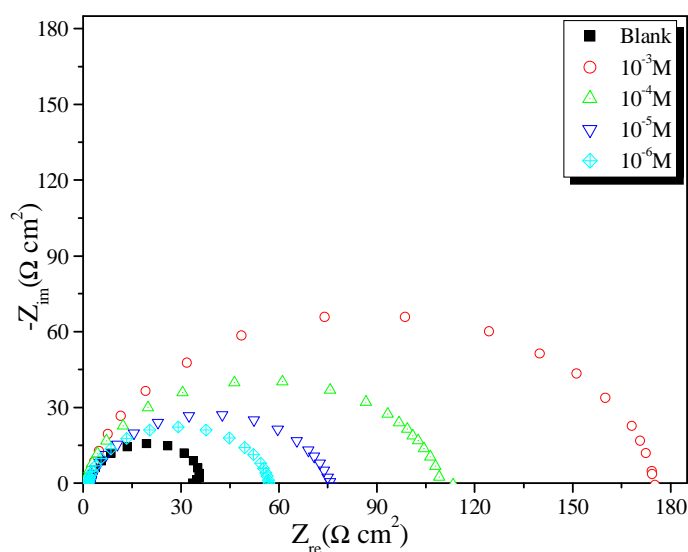


Figure 6. Nyquist diagrams mild steel in 1.0 M HCl without and with different concentrations of GP1.

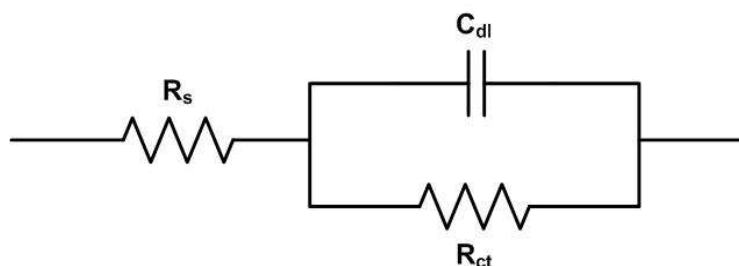
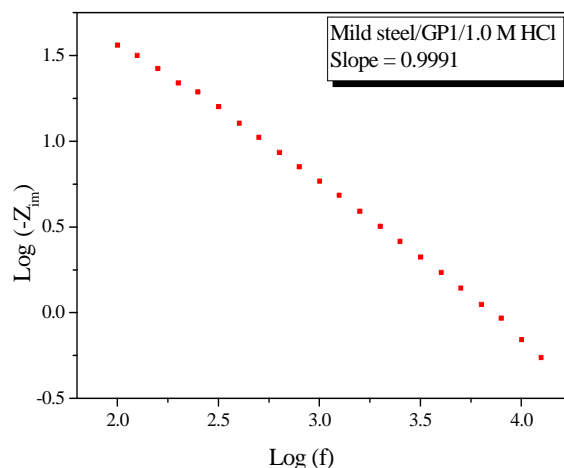


Figure 7. The electrochemical equivalent circuit used to fit the impedance measurements.

Table 4 Impedance parameters of mild steel in 1.0 M HCl containing different concentrations of GP1 compound at 305 K.

Inhibitor	Conc (M)	R_{ct} ($\Omega \text{ cm}^2$)	f_{max} (Hz)	C_{dl} ($\mu\text{F}/\text{cm}^2$)	η_z (%)
Blank	1.0	33.23	50.00	95.8	----
	10^{-3}	174.41	17.86	51.1	80.9
	10^{-4}	110.10	22.32	64.8	69.8
GP1	10^{-5}	75.08	28.09	75.5	55.7
	10^{-6}	56.19	28.09	100.9	40.9

It is necessary to plot the curves of variation of the logarithm of the imaginary impedance ($-Z_{im}$) versus the logarithm of frequency for this inhibitor at 10^{-3}M , to remove the phenomenon of diffusion is a result of any event Warburg [39]. From Fig.8, we note that the capacitive loops are all related to the charge transfer, who is confirmed by the value of the slope of each loop is approximately equal to unity.

Figure 8. Change $\text{Log}(-Z_{im})$ versus the logarithm of the frequency for the interface mild steel / 10^{-3}M / 1.0 M HCl.

Polarization curves

The potentiodynamic polarization measurements were carried out to study the kinetics of the cathodic and anodic reactions. Figure 9 shows the results of the effect of pyridazine derivative inhibitor on the cathodic as well as anodic polarization curves of mild steel in 1.0 M HCl respectively. It is evident from the figure that both reactions were suppressed with the addition of this inhibitor. This suggests that pyridazine derivative reduced the anodic dissolution reactions as well as retarded the hydrogen evolution reactions on the cathodic sites. Electrochemical corrosion kinetic parameters namely corrosion potential (E_{corr}), corrosion current density (I_{corr}) anodic and cathodic Tafel slopes (β_a and β_c) obtained from the extrapolation of the polarization curves are listed in Table 5.

It is seen that the addition of our inhibitor affects the polarization curves and consequently decreases I_{corr} significantly, due to increase in the blocked fraction of electrode surface by adsorption. Cathodic curves gave rise to parallel Tafel lines indicating that the hydrogen evolution is activation controlled and the reduction mechanism is not affected by the presence of inhibitor. In another hand, we note that the addition of product did not change the corrosion potential values (E_{corr}) for all concentration. These results demonstrated that the hydrogen evolution reaction was inhibited and that the inhibition efficiency increased with inhibitor concentration.

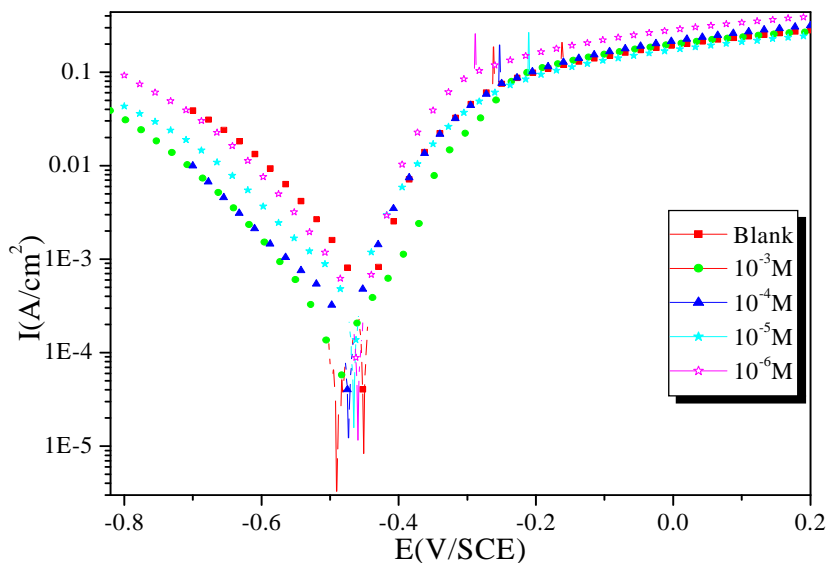


Figure 9. Polarization curves of mild steel in 1.0 M HCl containing different concentrations of GP1.

Table 5. Polarization data of mild steel in 1.0 M HCl without and with addition of inhibitor at 308 K.

Inhibitor	Conc (M)	$-E_{\text{corr}}$ (mV/SCE)	$-\beta_c$ (mV/dec)	I_{corr} ($\mu\text{A}/\text{cm}^2$)	η_{Tafel} (%)
Blank	1.0	455.2	127.3	815.7	-----
	10^{-3}	491.5	121.6	157.5	80.7
Ind2	10^{-4}	477.5	138.6	252.3	69.1
	10^{-5}	470.9	130.6	368.0	54.9
	10^{-6}	463.7	113.5	486.6	40.3

It is evident from Table 5 that the corrosion current density (I_{corr}) decreased by the increase in the adsorption of the inhibitor with increasing inhibitor concentration. According to Ferreira et.al [40] and Li et. al. [41], if the displacement in corrosion potential is more than 85 mV with respect to the corrosion potential of the blank solution, the inhibitor can be consider as a cathodic or anodic type. In present study, maximum displacement was 36 mV with respect to the corrosion potential of the uninhibited sample which indicates that the studied inhibitor is a mixed type of inhibitor.

Mechanism of Inhibition

Corrosion inhibition of mild steel in 1.0 M HCl by GP1 can be explained on the basis of molecular adsorption of inhibitor on to the metal surface. It is generally considered that the first step in the corrosion inhibition of a metal is the adsorption of the inhibitor molecules at metal / solution interface [42]. Organic compounds are adsorbed on the metal surface by (a) electrostatic interaction between the charged molecules and charged metal; (b) interaction of π -electrons with the metal; (c) interaction of unshared pair of electrons in the molecule with the metal; and (d) the combination of the all the effects [43,44].

CONCLUSION

All the measurements showed that the GP1 has excellent inhibition properties against the mild steel corrosion in hydrochloric acid solution. Inhibition efficiency of this inhibitor decreases with increase in temperature and further it leads to an increase in activation energy. The inhibitor follows the Langmuir adsorption isotherm in the process of adsorption. EIS measurements also indicates that the inhibitor performance increase due to the adsorption of molecule on the metal surface. Potentiodynamic polarization measurements showed that the inhibitor acts as mixed type of inhibitor. The inhibitor showed maximum inhibition efficiency at 1.0 mM concentration of the studied inhibitor. The inhibition efficiencies determined by EIS, potentiodynamic polarization and weight loss studies are in good agreement.

REFERENCES

- [1] A. Zarrouk, H. Zarrok, R. Salghi, B. Hammouti, F. Bentiss, R. Touir, M. Bouachrine, *J. Mater. Environ. Sci.*, **2013**, 4, 177.
- [2] M. Yadav, S. Kumar, U. Sharma, P.N. Yadav, *J. Mater. Environ. Sci.*, 2013, 4 (5), 691.
- [3] A. K. Singh, M. A. Quraishi, *J. Mater. Environ. Sci.*, **2010**, 1, 101.
- [4] U.J. Naik, V.A. Panchal, A.S. Patel, N.K. Shah, *J. Mater. Environ. Sci.*, **2012**, 3, 935.
- [5] D. Ben Hmamou, R. Salghi, A. Zarrouk, H. Zarrok, S.S. Al-Deyab, O. Benali, B. Hammouti, *Int. J. Electrochem. Sci.*, **2012**, 7, 8988.
- [6] B. Hammouti, A. Zarrouk, S.S. Al-Deyab and I. Warad, *Orient. J. Chem.*, 27 (**2011**) 23.
- [7] A. Zarrouk, M. Messali, H. Zarrok, R. Salghi, A.A. Ali, B. Hammouti, S.S. Al-Deyab, F. Bentiss, *Int. J. Electrochem. Sci.*, **2012**, 7, 6998.
- [8] H. Zarrok, A. Zarrouk, R. Salghi, Y. Ramli, B. Hammouti, S. S. Al-Deyab, E. M. Essassi, H. Oudda, *Int. J. Electrochem. Sci.*, **2012**, 7, 8958.
- [9] A. Zarrouk, B. Hammouti, S.S. Al-Deyab, R. Salghi, H. Zarrok, C. Jama, F. Bentiss, *Int. J. Electrochem. Sci.*, **2012**, 7, 5997.
- [10] D. Ben Hmamou, M. R. Aouad, R. Salghi, A. Zarrouk, M. Assouag, O. Benali, M. Messali, H. Zarrok, B. Hammouti, *J. Chem. Pharm. Res.*, **2012**, 4, 3489.
- [11] A. Zarrouk, H. Zarrok, R. Salghi, B. Hammouti, S.S. Al-Deyab, R. Touzani, M. Bouachrine, I. Warad, T. B. Hadda, *Int. J. Electrochem. Sci.*, **2012**, 7, 6353.
- [12] H. Zarrok, R. Saddik, H. Oudda, B. Hammouti, A. El Midaoui, A. Zarrouk, N. Benchat, M. Ebn Touhami, *Der Pharm. Chem.*, **2011**, 3, 272.
- [13] A. Zarrouk, B. Hammouti, A. Dafali, H. Zarrok, *Der Pharm. Chem.*, **2011**, 3, 266.
- [14] A. Ghazoui, R. Saddik, N. Benchat, B. Hammouti, M. Guenbour, A. Zarrouk, M. Ramdani, *Der Pharm. Chem.*, **2012**, 4, 352.
- [15] A. Zarrouk, B. Hammouti, H. Zarrok, M. Bouachrine, K.F. Khaled, S.S. Al-Deyab, *Int. J. Electrochem. Sci.*, **2012**, 6, 89.
- [16] A. Zarrouk, B. Hammouti, H. Zarrok, I. Warad, M. Bouachrine, *Der Pharm. Chem.*, **2011**, 3, 263.
- [17] A. H. Al Hamzi, H. Zarrok, A. Zarrouk, R. Salghi, B. Hammouti, S. S. Al-Deyab, M. Bouachrine, A. Amine, F. Guenoun, *Int. J. Electrochem. Sci.*, **2013**, 8, 2586.
- [18] A. Ghazoui, N. Bencacht, S. S. Al-Deyab, A. Zarrouk, B. Hammouti, M. Ramdani, M. Guenbour, *Int. J. Electrochem. Sci.*, **2013**, 8, 2272.
- [19] A. Zarrouk, H. Zarrok, R. Salghi, N. Bouroumane, B. Hammouti, S. S. Al-Deyab, R. Touzani, *Int. J. Electrochem. Sci.*, **2012**, 7, 10215.
- [20] H. Bendaha, A. Zarrouk, A. Aouniti, B. Hammouti, S. El Kadiri, R. Salghi, R. Touzani, *Phys. Chem. News*, **2012**, 64, 95.
- [21] D. Ben Hmamou, R. Salghi, A. Zarrouk, B. Hammouti, S.S. Al-Deyab, Lh. Bazzi, H. Zarrok, A. Chakir, L. Bammou, *Int. J. Electrochem. Sci.*, **2012**, 7, 2361
- [22] S.A. Umoren, I.B. Obot and E.E. Ebenso, *E-Journal of Chemistry*, **2008**, 5, 355.
- [23] A. K. Mishra and R. Balasubramaniam, *Mater. Chem. Phys.*, **2007**, 103, 385.
- [24] F. Bentiss, M. Lebrini, M. Traisnel, M. Lagrenee, *J. Appl. Electrochem.*, **2009**, 39, 1399.
- [25] M.A. Quraishi, S.K. Shukla, *Mater. Chem. Phys.*, **2009**, 113, 685.
- [26] I.B. Obot, N.O. Obi-Egbedi, S.A. Umoren, E.E. Ebenso, *Int. J. Electrochem. Sci.*, **2010**, 5, 994.
- [27] N. Benchat, E.M. Rakib, S. Abouricha, M. Alaoui, H. Allouchi, B. El Bali, *Synth. Commun.*, **2005**, 35, 2213.
- [28] H. Al Bay, A. Anafloos, S. Abouricha, A. Asahraou, N. Benchat, *Rev. Microbiol. Ind. San et Environn.*, **2008**, 2, 35.
- [29] M. Larif, A. Elmidaoui, A. Zarrouk, H. Zarrok, R. Salghi, B. Hammouti, H. Oudda, F. Bentiss, *Res. Chem. Intermed.*, **2012** DOI 10.1007/s11164-012-0788-2.
- [30] T. Szauer, A. Brandt, *Electrochim Acta*, **1981**, 26, 1253.
- [31] A.H. Mehaute, G. Greppe, *Solid State Ionics*, **1989**, 9, 17.
- [32] K.B. Samardzija, C. Lupu, N. Hackerman, A. R. Barron, *J. Mater. Chem.*, **2005**, 15, 1908.
- [33] F.M. Donahue, K. Nobe, *J. Electrochem. Soc.*, **1965**, 112, 886.
- [34] E. Kamis, F. Bellucci, R.M. Latanision, E.S.H. El-Ashry, *Corrosion*, **1991**, 47, 677.
- [35] M. Ozcan, R. Solmaz, G. Kardas, I. Dehri, *Colloid Surf. A.*, **2008**, 325, 57.
- [36] S.K. Shukla, M.A. Quraishi, *Corros. Sci.*, (**2010**) 52, 314.
- [37] S.K. Shukla, M.A. Quraishi, *Corros. Sci.*, (**2009**) 51, 1990.
- [38] F. Bentiss, M. Traisnel, M. Lagrenee, *Corros. Sci.*, (2000, 42, 127.
- [39] A. Zarrouk, *PhD thesis*, Faculty of Sciences, Oujda, Morocco (**2011**).
- [40] E.S. Ferreira, C. Giancomelli, F.C. Giacomelli, A. Spinelli, *Mater. Chem. Phys.*, **2004**, 83, 129.
- [41] W.H. Li, Q. He, C.L. Pei, B.R. Hou, *J. Appl. Electrochem.*, **2008**, 38, 289.

[42] M. Sahin, S. Bilgic, H. Yilmaz, *Appl. Surf. Sci.*, **2002**, 195, 1.

[43] H. Shorky, M. Yuasa, I. Sekine, R.M. Issa, H.Y. El-Baradie, G.K. Gomma, *Corros. Sci.*, **1998**, 40, 2173.

[44] D.P. Schweinsberg, G.A. George, A.K. Nanayakkara, D.A. Steiner, *Corros. Sci.*, **1988**, 28, 33.